



OPEN

Spin effect on the low-temperature resistivity maximum in a strongly interacting 2D electron system

A. A. Shashkin¹, M. Yu. Melnikov¹, V. T. Dolgoplov¹, M. M. Radonjić², V. Dobrosavljević³, S.-H. Huang⁴, C. W. Liu⁴, Amy Y. X. Zhu⁵ & S. V. Kravchenko⁵✉

The increase in the resistivity with decreasing temperature followed by a drop by more than one order of magnitude is observed on the metallic side near the zero-magnetic-field metal-insulator transition in a strongly interacting two-dimensional electron system in ultra-clean SiGe/Si/SiGe quantum wells. We find that the temperature T_{\max} , at which the resistivity exhibits a maximum, is close to the renormalized Fermi temperature. However, rather than increasing along with the Fermi temperature, the value T_{\max} decreases appreciably for spinless electrons in spin-polarizing (parallel) magnetic fields. The observed behaviour of T_{\max} cannot be described by existing theories. The results indicate the spin-related origin of the effect.

The zero-magnetic-field metal-insulator transition has been reported in a number of strongly-correlated two-dimensional (2D) electron systems in semiconductors^{1–14}, in quasi-2D organic charge-transfer salts (Mott organics)¹⁵, as well as in 2D transition metal dichalcogenides^{16–18}. The hallmark of the low-temperature resistivity ρ on the metallic side near the metal-insulator transition is a non-monotonic $\rho(T)$: when the temperature is decreased, the resistivity first increases, reaching a maximum at a temperature T_{\max} , and then drops at lower temperatures. The strength of such a resistivity drop varies from system to system, reaching a 12-fold value in ultra-pure SiGe/Si/SiGe quantum wells¹²; note that this is in contrast to the case of low-mobility Si/SiGe quantum wells where the resistivity decreases at low temperatures by a factor of about 1.5 and the disorder effects are dominant^{19,20}. The increase of the effective mass with decreasing electron density^{8,9,13,14,21–24} suggests that the effect of strong electron-electron interactions is the main driving force for the experimentally observed metal-insulator transition due to the fermion condensation^{24,25} or the Wigner-Mott transition^{26,27}. From the theoretical standpoint, the dynamical mean-field theory (DMFT) approach^{26,28,29} has provided a successful quantitative description of the low-temperature resistivity drop in zero magnetic field in all these systems, especially in SiGe/Si/SiGe quantum wells³⁰. Over a wide range of electron densities, the experimental ratio $(\rho(T) - \rho(0))/(\rho(T_{\max}) - \rho(0))$ has been found to be a universal function of T/T_{\max} , which is consistent with the DMFT. According to this theory, T_{\max} corresponds to the quasiparticle coherence temperature, which is of the order of the Fermi temperature T_F determined by the effective electron mass renormalized by interactions: $T_{\max} \sim T_F$. Below this temperature, the elastic electron-electron scattering corresponds to coherent transport, while at higher temperatures, the inelastic electron-electron scattering becomes strong and gives rise to a fully incoherent transport. Notably, similar functional form of the resistivity $\rho(T)$ can be expected within the screening theory in its general form (for more on this, see Ref. ³⁰). Similar non-monotonic $\rho(T)$ dependence with a maximum at $T_{\max} \sim T_F$ is predicted by another approach based on the Pomeranchuk effect expected within a phase coexistence region between the Wigner crystal and a Fermi liquid^{31–33}. Finally, the renormalization-group scaling theory, which takes account of the existence of multiple valleys in the electron spectrum^{34,35}, allows for a quantitative description of non-monotonic $\rho(T)$ on the metallic side in the close vicinity of the metal-insulator transition for the resistivities low compared to $\pi h/e$ ²⁰. Within this theory, T_{\max} is determined by the competition between electron-electron interactions and disorder, the value of T_{\max} being much smaller than T_F and decreasing when lifting the spin degeneracy.

¹Institute of Solid State Physics, Chernogolovka, Moscow District 142432, Russia. ²Institute of Physics Belgrade, University of Belgrade, Pregrevice 118, 11080 Belgrade, Serbia. ³Department of Physics and National High Magnetic Field Laboratory, Florida State University, Tallahassee, FL 32306, USA. ⁴Department of Electrical Engineering and Graduate Institute of Electronics Engineering, National Taiwan University, Taipei 106, Taiwan. ⁵Department of Physics, Northeastern University, Boston, MA 02115, USA. ✉email: s.kravchenko@northeastern.edu

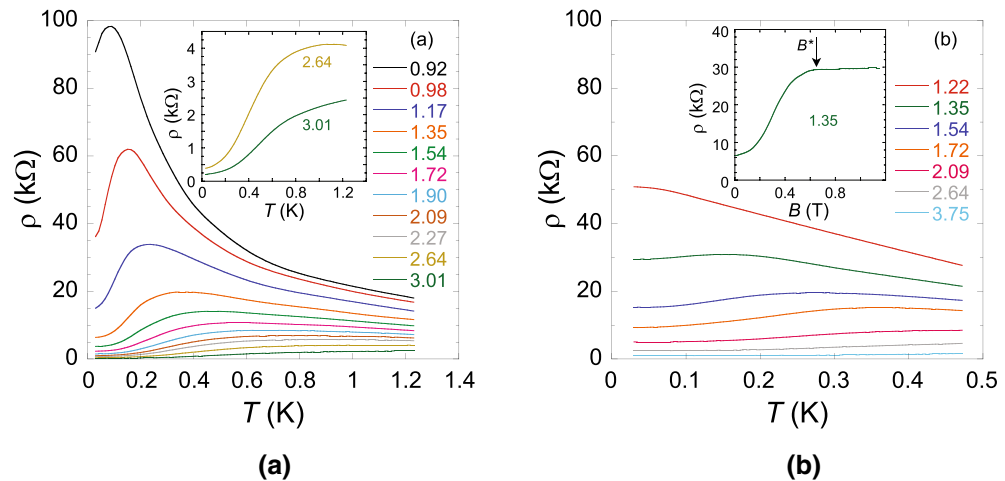


Figure 1. Non-monotonic temperature dependences of the resistivity of the 2D electron system in SiGe/Si/SiGe quantum wells on the metallic side near the metal-insulator transition (a) in $B = 0$ and (b) in $B = B^*$; the magnetic fields used are spanned in the range between approximately 1 and 2 T. The electron densities are indicated in units of 10^{10} cm^{-2} . The inset in (a) shows $\rho(T)$ at $n_s = 2.64$ and $3.01 \times 10^{10} \text{ cm}^{-2}$ on an expanded scale. The inset in (b) shows the parallel-field magnetoresistance at $n_s = 1.35 \times 10^{10} \text{ cm}^{-2}$ at $T \approx 25 \text{ mK}$. The polarization field B^* is indicated.

The existence of the metallic state in strongly interacting 2D electron systems is intimately related to the existence of spin and valley degrees of freedom^{34–37}. If the electron spins become completely polarized by a magnetic field B^* parallel to the 2D plane, the spin degeneracy that determines the Fermi energy changes to $g_s = 1$, corresponding to spinless electrons. In a thin 2D electron system in the metallic regime, the resistivity increases with parallel magnetic field by a factor of a few and saturates above the polarization field B^* ^{38–45}. (An attempt was made by M. S. Hossain *et al.*⁴⁶ to analyze the data for B^* in the insulating phase. However, such data reflect the physics of localized electron moments in the band tail, which is entirely different from that of the metallic phase (see, *e.g.*, Ref. 9), and, therefore, the conclusion of M. S. Hossain *et al.* on the ferromagnetic state is not justified.) The metallic temperature dependence of the resistivity is suppressed in the spin-polarized regime, as observed in silicon metal-oxide-semiconductor field-effect transistors (MOSFETs)^{38,43,47}, *p*-type GaAs/AlGaAs heterostructures^{42,45}, and narrow AlAs quantum wells⁴⁴. Recent work has established that the ultra-clean 2D electron system in SiGe/Si/SiGe quantum wells, which is similar to the clean Si MOSFETs in that the 2D electrons host in Si but is distinguished mainly by the much higher electron mobility, still exhibits a metal-insulator transition even at $B = B^*$ that is determined using a number of different measurement methods^{9,43} and is attributed to the existence of two distinct valleys in its spectrum⁴⁸.

In this paper, we report studies of the non-monotonic temperature dependence of the resistivity on the metallic side near the metal-insulator transition in a strongly interacting, spin-unpolarized ($g_s = 2$) as well as fully spin-polarized (or spinless, $g_s = 1$) bi-valley 2D electron system in ultra-clean SiGe/Si/SiGe quantum wells. We find that in zero magnetic field, the temperature T_{max} , at which the resistivity has a maximum, is close to the renormalized Fermi temperature T_F , which is in agreement with the dynamical mean-field theory. However, rather than increasing along with the Fermi temperature, the value T_{max} decreases appreciably for spinless electrons in spin-polarizing magnetic fields, which is in contradiction with this theory. A scaling analysis of $\rho(T)$ in the spinless electron system in the spirit of DMFT shows that the low-temperature resistivity drop is still described by the theory, similar to the case of the spin-unpolarized electron system. At the same time, the reduced value of T_{max} in spin-polarizing magnetic fields is consistent with the predictions of the renormalization-group scaling theory, but T_{max} in zero magnetic field is in disagreement with this theory. Thus, the observed behaviour of T_{max} cannot be described by existing theories. Nor can it be explained in terms of the increase of the residual disorder potential and the reduction of the electron interaction strength due to the reduced spin degrees of freedom in spin-polarizing magnetic fields, because the relation $T_{\text{max}} \sim T_F$ still holds for clean Si MOSFETs^{28,29} and low-mobility Si/SiGe quantum wells²⁰ in zero magnetic field. This indicates the spin-related origin of the effect.

Raw data for the resistivity as a function of temperature are shown at zero magnetic field ($g_s = 2$) in Fig. 1a and at $B = B^*$ ($g_s = 1$) in Fig. 1b for electron densities above the critical electron densities for the metal-insulator transition $n_c(0) \approx 0.88 \times 10^{10} \text{ cm}^{-2}$ and $n_c(B^*) \approx 1.1 \times 10^{10} \text{ cm}^{-2}$, respectively. In zero magnetic field, the $\rho(T)$ curves are non-monotonic with the maxima at density-dependent temperatures $T_{\text{max}}(0)$ over a wide range of electron densities n_s ; below $T_{\text{max}}(0)$, the resistivity drops sharply with decreasing temperature so that the drop can exceed an order of magnitude (see the inset to Fig. 1a). At $B = B^*$, the $\rho(T)$ curves are non-monotonic in a narrower range of electron densities, and the resistivity drop below $T_{\text{max}}(B^*)$ weakens. The values of B^* are density-dependent and have been determined by the saturation of the $\rho(B)$ dependences (see the inset to Fig. 1b), which corresponds to the lifting of the spin degeneracy^{40,41}. Magnetic fields used in our experiments were within the range between approximately 1 and 2 T. The measurements were restricted to 0.5 K because this was the

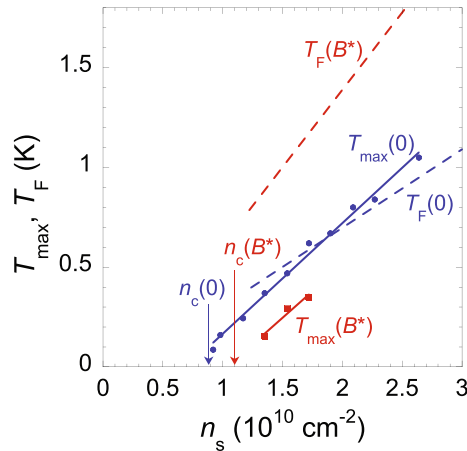


Figure 2. T_{\max} as a function of electron density in $B = 0$ (circles) and in $B = B^*$ (squares). Solid lines are linear fits. Critical electron densities for the metal-insulator transition in $B = 0$ and $B = B^*$ are indicated. Dashed lines show the Fermi temperatures T_F in $B = 0$ and $B = B^*$ calculated using the low-temperature value B^* and Eq. (1), see text.

highest temperature at which the complete spin polarization could still be achieved; the restriction is likely to reflect the degeneracy condition for the dilute electron system with low Fermi energy.

In Fig. 2, which is the main figure of this paper, we plot the values of T_{\max} as a function of the electron density in $B = 0$ and $B = B^*$. The data for $T_{\max}(B^*)$ lie significantly lower than those for $T_{\max}(0)$. Interestingly, each dependence can be described by a linear function that extrapolates to zero at n_s close to $n_c(0)$ or $n_c(B^*)$, and the slopes of both dependences are close to each other. We also plot the calculated values of renormalized Fermi temperatures T_F for both cases. In zero magnetic field, the density dependences of the resistivity maximum temperature $T_{\max}(0)$ and the Fermi temperature $T_F(0)$ are close to each other in the electron density range where they overlap. However, there is a qualitative difference between the behaviour of T_{\max} and that of T_F when lifting the spin degeneracy. Rather than increasing along with the Fermi temperature, the value T_{\max} decreases when polarizing electron spins.

The Fermi temperature $T_F(B^*)$ has been calculated from the low-temperature value B^* (see the inset to Fig. 1b) based on the equality of the Fermi energy of completely spin-polarized electrons and the Zeeman energy in the polarization field B^* ²⁴:

$$k_B T_F(B^*) = \frac{2\pi \hbar^2 n_s}{g_v m} = g_F \mu_B B^*, \tag{1}$$

where k_B is the Boltzmann constant, $g_v = 2$ is the valley degeneracy, m is the renormalized energy-averaged effective mass that is determined by the density of states, $g_F \approx g_0 = 2$ is the g -factor at the Fermi level, g_0 is the g -factor in bulk silicon, and μ_B is the Bohr magneton. We argue that the Fermi temperature $T_F(0)$ of spin-unpolarized electrons is approximately half of the Fermi temperature $T_F(B^*)$ of completely spin-polarized ones. Indeed, it was experimentally shown in Ref. 49 that the electron spin magnetization is proportional to the parallel magnetic field in the range up to $B = B^*$ for the clean, strongly interacting 2D electron system in Si MOSFETs that is similar to the 2D electron system in SiGe/Si/SiGe quantum wells. (For strongly disordered Si MOSFETs, the band tail of localized electrons persists into the metallic regime⁵⁰ in which case both the nonlinear magnetization as a function of parallel magnetic field and the shift of the dependence $B^*(n_s)$ to higher densities are observed due to the presence of localized electron moments in the band tail^{9,51–54}.) Taking into account the smallness of the exchange effects in the 2D electron system in silicon so that the g -factor is approximately constant close to $g_0 = 2$ at low densities^{8,9,24}, this indicates that the renormalized density of states in a spin subband is approximately constant below the Fermi level, independent of the magnetic field. Therefore, the change of T_F when lifting the spin degeneracy should be controlled by the change of g_s . As concerns the band flattening corresponding to a peak in the density of states at the Fermi level, observed in the 2D electron system in SiGe/Si/SiGe quantum wells, the Fermi energy is not particularly sensitive to this flattening, at least, not too close to the critical point²⁴. So, one expects that the relation $T_F(0) \approx T_F(B^*)/2$ holds for the data in question. We stress that its accuracy is not crucial for our qualitative results.

In Fig. 3, we plot the ratio $\delta\rho/\delta\rho_{\max} = (\rho(T) - \rho(0))/(\rho(T_{\max}) - \rho(0))$ as a function of T/T_{\max} in $B = B^*$ so as to check the applicability of the DMFT. The curve for the highest electron density follows the theoretical dependence in the weak-disorder limit at all temperatures. Two other curves for lower electron densities also follow the theoretical dependence at $T \leq T_{\max}$ but deviate from the theory at higher temperatures, revealing the behaviour similar to that observed at low n_s in zero magnetic field³⁰. Albeit the density range of the applicability of DMFT to the completely spin-polarized system is not as wide as that in $B = 0$, the low-temperature resistivity drop is described by the theory, similar to the case of the spin-unpolarized electron system. For completeness, in the inset to Fig. 3 we plot the ratio ρ/ρ_{\max} in the fully spin-polarized system as a function of

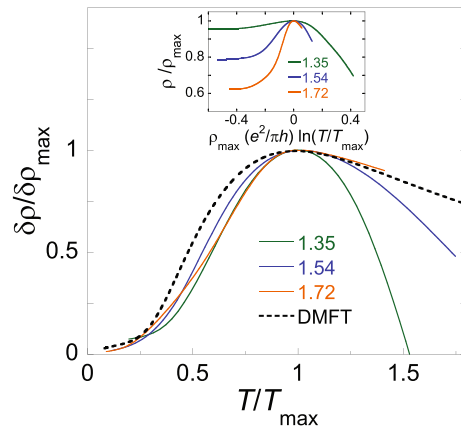


Figure 3. The ratio $\delta\rho/\delta\rho_{\max}$ plotted as a function of T/T_{\max} in $B = B^*$. The electron densities are indicated in units of 10^{10} cm^{-2} . The dashed line is the result of DMFT in the weak-disorder limit^{26,28,29}. The inset shows the analysis based on the scaling form suggested by the renormalization-group scaling theory^{34,35}.

$\rho_{\max}(e^2/\pi h)\ln(T/T_{\max})$, which is the scaling form suggested by the renormalization-group scaling theory^{34,35}. The data do not scale in the range of electron densities studied.

The dynamical mean-field theory successfully describes the closeness of T_{\max} and the renormalized Fermi temperature T_F in zero magnetic field, as well as the resistivity drop at temperatures below T_{\max} in both spin-unpolarized and fully spin-polarized electron systems. However, the observed decrease of T_{\max} when lifting the spin degeneracy is opposite to the predictions of DMFT. At the same time, the reduced value of T_{\max} in spin-polarizing magnetic fields is consistent with the predictions of the renormalization-group scaling theory, but T_{\max} in zero magnetic field is in disagreement with this theory. The observed behaviour of T_{\max} cannot be described by existing theories.

In view of the competition between electron-electron interactions and disorder, one can expect the value T_{\max} to decrease with increasing disorder level or decreasing electron interaction strength, as occurs in our case when lifting the spin degeneracy. However, the increase of the residual disorder potential when lifting the spin degeneracy in SiGe/Si/SiGe quantum wells, manifested in the metallic regime by the resistivity increase by a factor of a few (the inset to Fig. 1b), cannot be the origin for the observed weakening of the resistivity drop at temperatures below T_{\max} and shift of the maximum in $\rho(T)$ to lower temperatures. Indeed, we compare to the electron system of clean Si MOSFETs, which is different from the studied SiGe/Si/SiGe electron system mainly by lower electron mobility, whereas at the $B = 0$ metal-insulator transition in both systems, the values of the interaction parameter are similar, $r_s \approx 20$ (for details, see Ref. 12); the interaction parameter is defined as the ratio between the Coulomb and (bare) Fermi energies, $r_s = g_s g_v / 2(\pi n_s)^{1/2} a_B$ (where a_B is the effective Bohr radius in semiconductor). Importantly, both systems correspond to the clean limit where the electron interactions are dominant over disorder effects, which is the regime we are interested in. In this case, the zero-magnetic-field metal-insulator transition occurs close to the electron density at which the effective mass at the Fermi level tends to diverge¹². In clean Si MOSFETs, where the electron mobility is some two orders of magnitude lower than that in SiGe/Si/SiGe quantum wells studied here, the resistivity drop at $T < T_{\max}$ in zero magnetic field reaches a factor of 7, which is comparable to that in our samples. Also, in clean Si MOSFETs, the positions of the $\rho(T)$ maxima in $B = 0$ closely follow the renormalized Fermi temperatures^{28,29}, which is similar to our finding in $B = 0$. Neither can the reduction of the electron interaction strength due to the reduced spin degrees of freedom in spin-polarizing magnetic fields be the origin of the observed behaviour of T_{\max} . Indeed, the relation $T_{\max} \sim T_F$ still holds for low-mobility Si/SiGe quantum wells in zero magnetic field at electron densities above $n_s \approx 10^{11} \text{ cm}^{-2}$ ²⁰, which corresponds to the interaction parameter smaller by a factor of a few compared to that in our range of electron densities. This indicates the spin-related origin of the behaviour of T_{\max} observed in our samples.

It is worth noting that the suppression of the metallic regime and the increase of the transition point when lifting the spin degeneracy in a strongly correlated 2D electron system (see, e.g., Fig. 2, as well as earlier experimental data^{43,55–57}) are explained taking account of the spin and valley degrees of freedom, according to theories^{34–37,58,59}. Similarly, within the DMFT, the critical density is predicted to increase in spin-polarizing magnetic fields²⁶.

In conclusion, we have studied the non-monotonic temperature dependence of the resistivity on the metallic side near the metal-insulator transition in a strongly interacting, spin-unpolarized and spinless two-valley 2D electron system in ultra-clean SiGe/Si/SiGe quantum wells. We have found that in zero magnetic field, the resistivity maximum temperature T_{\max} is close to the renormalized Fermi temperature T_F , which is in agreement with the dynamical mean-field theory. However, rather than increasing along with the Fermi temperature, the value T_{\max} decreases appreciably for spinless electrons in spin-polarizing magnetic fields, which is in contradiction with the theory. The DMFT quantitatively describes the low-temperature resistivity drop in both spin-unpolarized and spinless electron systems. At the same time, the reduced value of T_{\max} in spin-polarizing magnetic fields is consistent with the predictions of the renormalization-group scaling theory, but T_{\max} in zero magnetic field is in disagreement with this theory. Thus, the observed behaviour of T_{\max} cannot be described by existing theories. Nor can it be explained in terms of the increase of the residual disorder potential and the reduction of the electron

interaction strength due to the reduced spin degrees of freedom in spin-polarizing magnetic fields, because the relation $T_{\max} \sim T_F$ still holds for clean Si MOSFETs and low-mobility Si/SiGe quantum wells in zero magnetic field, indicating the spin-related origin of the effect. To describe the observed behaviour of T_{\max} within a single approach that treats properly the spin effects on the low-temperature resistivity in a strongly interacting 2D electron system in parallel magnetic fields, further theoretical efforts are necessary.

Methods

The samples we used were ultra-high mobility SiGe/Si/SiGe quantum wells. The peak electron mobility in these samples reaches $240 \text{ m}^2/\text{Vs}$. The approximately 15 nm wide silicon (001) quantum well was sandwiched between $\text{Si}_{0.8}\text{Ge}_{0.2}$ potential barriers. The samples were patterned in Hall-bar shapes with the distance between the potential probes of $150 \mu\text{m}$ and width of $50 \mu\text{m}$ using standard photo-lithography. The long side of the Hall bar corresponded to the direction of current parallel to the $[110]$ or $[\bar{1}10]$ crystallographic axis. The in-plane magnetic field was perpendicular to the current to exclude the influence of ridges on the quantum well surface on the resistance measured at high electron densities (for more details, see Refs. ^{60,61}). Measurements were carried out in an Oxford TLM-400 dilution refrigerator with a base temperature of $\approx 25 \text{ mK}$. Data were taken by a standard four-terminal lock-in technique in a frequency range $0.5\text{--}11 \text{ Hz}$ in the linear regime of response.

Data availability

The data that support the findings of this study are available from the corresponding author upon reasonable request.

Received: 4 January 2022; Accepted: 16 March 2022

Published online: 24 March 2022

References

1. Kravchenko, S. V., Kravchenko, G. V., Furneaux, J. E., Pudalov, V. M. & DiIorio, M. Possible metal-insulator transition at $B = 0$ in two dimensions. *Phys. Rev. B* **50**, 8039–8042 (1994).
2. Popović, D., Fowler, A. B. & Washburn, S. Metal-insulator transition in two dimensions: effects of disorder and magnetic field. *Phys. Rev. Lett.* **79**, 1543–1546 (1997).
3. Coleridge, P. T., Williams, R. L., Feng, Y. & Zawadzki, P. Metal-insulator transition at $B = 0$ in p -type SiGe. *Phys. Rev. B* **56**, R12764–R12767 (1997).
4. Hanein, Y. *et al.* The metalliclike conductivity of a two-dimensional hole system. *Phys. Rev. Lett.* **80**, 1288–1291 (1998).
5. Hanein, Y. *et al.* Observation of the metal-insulator transition in two-dimensional n -type GaAs. *Phys. Rev. B* **58**, R13338–R13340 (1998).
6. Papadakis, S. J. & Shayegan, M. Apparent metallic behavior at $B = 0$ of a two-dimensional electron system in AlAs. *Phys. Rev. B* **57**, R15068–R15071 (1998).
7. Gao, X. P. A., Mills, A. P., Ramirez, A. P., Pfeiffer, L. N. & West, K. W. Weak-localization-like temperature-dependent conductivity of a dilute two-dimensional hole gas in a parallel magnetic field. *Phys. Rev. Lett.* **89**, 016801 (2002).
8. Kravchenko, S. V. & Sarachik, M. P. Metal-insulator transition in two-dimensional electron systems. *Rep. Prog. Phys.* **67**, 1–44 (2004).
9. Shashkin, A. A. Metal-insulator transitions and the effects of electron-electron interactions in two-dimensional electron systems. *Phys.-Usp.* **48**, 129–149 (2005).
10. Pudalov, V. M. Metal-insulator transitions and related phenomena in a strongly correlated two-dimensional electron system. *Phys.-Usp.* **49**, 203–208 (2006).
11. Kozuka, Y., Tsukazaki, A. & Kawasaki, M. Challenges and opportunities of ZnO-related single crystalline heterostructures. *Appl. Phys. Rev.* **1**, 011303 (2014).
12. Melnikov, M. Y. *et al.* Quantum phase transition in ultrahigh mobility SiGe/Si/SiGe two-dimensional electron system. *Phys. Rev. B* **99**, 081106(R) (2019).
13. Shashkin, A. A. & Kravchenko, S. V. Recent developments in the field of the metal-insulator transition in two dimensions. *Appl. Sci.* **9**, 1169 (2019).
14. Shashkin, A. A. & Kravchenko, S. V. Metal-insulator transition and low-density phases in a strongly-interacting two-dimensional electron system. *Ann. Phys.* **435**, 168542 (2021).
15. Dressel, M. & Tomić, S. Molecular quantum materials: electronic phases and charge dynamics in two-dimensional organic solids. *Adv. Phys.* **69**, 1–120 (2020).
16. Moon, B. H., Han, G. H., Radonjić, M. M., Ji, H. & Dobrosavljević, V. Quantum critical scaling for finite-temperature Mott-like metal-insulator crossover in few-layered MoS_2 . *Phys. Rev. B* **102**, 245424 (2020).
17. Moon, B. H. Metal-insulator transition in two-dimensional transition metal dichalcogenides. *Emerg. Mater.* **4**, 989–998 (2021).
18. Li, T. *et al.* Continuous Mott transition in semiconductor moiré superlattices. *Nature* **597**, 350–354 (2021).
19. Lai, K., Pan, W., Tsui, D. C. & Xie, Y.-H. Observation of the apparent metal-insulator transition of high-mobility two-dimensional electron system in a $\text{Si/Si}_{1-x}\text{Ge}_x$ heterostructure. *Appl. Phys. Lett.* **84**, 302–304 (2004).
20. Lu, T. M. *et al.* Termination of two-dimensional metallic conduction near the metal-insulator transition in a Si/SiGe quantum well. *Phys. Rev. Lett.* **107**, 126403 (2011).
21. Shashkin, A. A., Kravchenko, S. V., Dolgoplov, V. T. & Klapwijk, T. M. Sharp increase of the effective mass near the critical density in a metallic two-dimensional electron system. *Phys. Rev. B* **66**, 073303 (2002).
22. Mokashi, A. *et al.* Critical behavior of a strongly interacting 2D electron system. *Phys. Rev. Lett.* **109**, 096405 (2012).
23. Kuntsevich, A. Y., Tupikov, Y. V., Pudalov, V. M. & Burmistrov, I. S. Strongly correlated two-dimensional plasma explored from entropy measurements. *Nat. Commun.* **6**, 7298 (2015).
24. Melnikov, M. Y. *et al.* Indication of band flattening at the Fermi level in a strongly correlated electron system. *Sci. Rep.* **7**, 14539 (2017).
25. Amusia, M., Popov, K., Shaginyan, V. & Stefanowicz, W. *Theory of heavy-fermion compounds* (Springer, New York, 2015).
26. Camjayi, A., Haule, K., Dobrosavljević, V. & Kotliar, G. Coulomb correlations and the Wigner-Mott transition. *Nat. Phys.* **4**, 932–935 (2008).
27. Brussarski, P., Li, S., Kravchenko, S. V., Shashkin, A. A. & Sarachik, M. P. Transport evidence for a sliding two-dimensional quantum electron solid. *Nat. Commun.* **9**, 3803 (2018).
28. Radonjić, M. M., Tanasković, D., Dobrosavljević, V., Haule, K. & Kotliar, G. Wigner-Mott scaling of transport near the two-dimensional metal-insulator transition. *Phys. Rev. B* **85**, 085133 (2012).

29. Dobrosavljević, V. & Tanasković, D. Wigner-Mott quantum criticality: From 2D-MIT to ^3He and Mott organics. In Kravchenko, S. V. (ed.) *Strongly Correlated Electrons in Two Dimensions*, chap. 1, 1–46 (Pan Stanford Publishing, 2017).
30. Shashkin, A. A. *et al.* Manifestation of strong correlations in transport in ultraclean SiGe/Si/SiGe quantum wells. *Phys. Rev. B* **102**, 081119(R) (2020).
31. Spivak, B. Phase separation in the two-dimensional electron liquid in MOSFETs. *Phys. Rev. B* **67**, 125205 (2003).
32. Spivak, B. & Kivelson, S. A. Phases intermediate between a two-dimensional electron liquid and Wigner crystal. *Phys. Rev. B* **70**, 155114 (2004).
33. Spivak, B. & Kivelson, S. A. Transport in two dimensional electronic micro-emulsions. *Ann. Phys.* **321**, 2071–2115 (2006).
34. Punnoose, A. & Finkelstein, A. M. Dilute electron gas near the metal-insulator transition: role of valleys in silicon inversion layers. *Phys. Rev. Lett.* **88**, 016802 (2001).
35. Punnoose, A. & Finkelstein, A. M. Metal-insulator transition in disordered two-dimensional electron systems. *Science* **310**, 289–291 (2005).
36. Finkelstein, A. M. Influence of Coulomb interaction on the properties of disordered metals. *Sov. Phys. JETP* **57**, 97–108 (1983).
37. Lee, P. A. & Ramakrishnan, T. V. Disordered electronic systems. *Rev. Mod. Phys.* **57**, 287–337 (1985).
38. Simonian, D., Kravchenko, S. V., Sarachik, M. P. & Pudalov, V. M. Magnetic field suppression of the conducting phase in two dimensions. *Phys. Rev. Lett.* **79**, 2304–2307 (1997).
39. Pudalov, V. M., Brunthaler, G., Prinz, A. & Bauer, G. Instability of the two-dimensional metallic phase to a parallel magnetic field. *JETP Lett.* **65**, 932–937 (1997).
40. Okamoto, T., Hosoya, K., Kawaji, S. & Yagi, A. Spin degree of freedom in a two-dimensional electron liquid. *Phys. Rev. Lett.* **82**, 3875–3878 (1999).
41. Vitkalov, S. A., Zheng, H., Mertes, K. M., Sarachik, M. P. & Klapwijk, T. M. Small-angle Shubnikov-de Haas measurements in a 2D electron system: The effect of a strong in-plane magnetic field. *Phys. Rev. Lett.* **85**, 2164–2167 (2000).
42. Yoon, J., Li, C. C., Shahar, D., Tsui, D. C. & Shayegan, M. Parallel magnetic field induced transition in transport in the dilute two-dimensional hole system in GaAs. *Phys. Rev. Lett.* **84**, 4421–4424 (2000).
43. Shashkin, A. A., Kravchenko, S. V. & Klapwijk, T. M. Metal-insulator transition in a 2D electron gas: equivalence of two approaches for determining the critical point. *Phys. Rev. Lett.* **87**, 266402 (2001).
44. Vakili, K., Shkolnikov, Y. P., Tutuc, E., De Poortere, E. P. & Shayegan, M. Spin susceptibility of two-dimensional electrons in narrow AlAs quantum wells. *Phys. Rev. Lett.* **92**, 226401 (2004).
45. Gao, X. P. A. *et al.* Spin-polarization-induced tenfold magnetoresistivity of highly metallic two-dimensional holes in a narrow GaAs quantum well. *Phys. Rev. B* **73**, 241315(R) (2006).
46. Hossain, M. S. *et al.* Observation of spontaneous ferromagnetism in a two-dimensional electron system. *Proc. Natl. Acad. Sci. USA* **117**, 32244–32250 (2020).
47. Li, S. & Sarachik, M. P. Resistivity of the insulating phase approaching the two-dimensional metal-insulator transition: the effect of spin polarization. *Phys. Rev. B* **95**, 041301(R) (2017).
48. Melnikov, M. Y. *et al.* Metallic state in a strongly interacting spinless two-valley electron system in two dimensions. *Phys. Rev. B* **101**, 045302 (2020).
49. Shashkin, A. A. *et al.* Pauli spin susceptibility of a strongly correlated two-dimensional electron liquid. *Phys. Rev. Lett.* **96**, 036403 (2006).
50. Prus, O., Yaish, Y., Reznikov, M., Sivan, U. & Pudalov, V. Thermodynamic spin magnetization of strongly correlated two-dimensional electrons in a silicon inversion layer. *Phys. Rev. B* **67**, 205407 (2003).
51. Dolgoplov, V. T. & Gold, A. Comment on Weak anisotropy and disorder dependence of the in-plane magnetoresistance in high-mobility (100) Si-inversion layers. *Phys. Rev. Lett.* **89**, 129701 (2002).
52. Gold, A. & Dolgoplov, V. T. On the role of disorder in transport and magnetic properties of the two-dimensional electron gas. *J. Phys. Condens. Matter* **14**, 7091–7096 (2002).
53. Teneh, N., Kuntsevich, A. Y., Pudalov, V. M. & Reznikov, M. Spin-droplet state of an interacting 2D electron system. *Phys. Rev. Lett.* **109**, 226403 (2012).
54. Pudalov, V. M., Kuntsevich, A. Y., Gershenson, M. E., Burmistrov, I. S. & Reznikov, M. Probing spin susceptibility of a correlated two-dimensional electron system by transport and magnetization measurements. *Phys. Rev. B* **98**, 155109 (2018).
55. Dolgoplov, V. T., Kravchenko, G. V., Shashkin, A. A. & Kravchenko, S. V. Properties of electron insulating phase in Si inversion layers at low-temperatures. *JETP Lett.* **55**, 733–737 (1992).
56. Eng, K., Feng, X. G., Popović, D. & Washburn, S. Effects of a parallel magnetic field on the metal-insulator transition in a dilute two-dimensional electron system. *Phys. Rev. Lett.* **88**, 136402 (2002).
57. Jaroszyński, J., Popović, D. & Klapwijk, T. M. Magnetic-field dependence of the anomalous noise behavior in a two-dimensional electron system in silicon. *Phys. Rev. Lett.* **92**, 226403 (2004).
58. Fleury, G. & Waintal, X. Many-body localization study in low-density electron gases: Do metals exist in two dimensions?. *Phys. Rev. Lett.* **101**, 226803 (2008).
59. Dolgoplov, V. T., Shashkin, A. A. & Kravchenko, S. V. Spin polarization and exchange-correlation effects in transport properties of two-dimensional electron systems in silicon. *Phys. Rev. B* **96**, 075307 (2017).
60. Melnikov, M. Y. *et al.* Ultra-high mobility two-dimensional electron gas in a SiGe/Si/SiGe quantum well. *Appl. Phys. Lett.* **106**, 092102 (2015).
61. Melnikov, M. Y. *et al.* Unusual anisotropy of inplane field magnetoresistance in ultra-high mobility SiGe/Si/SiGe quantum wells. *J. Appl. Phys.* **122**, 224301 (2017).

Acknowledgements

The ISSP group was supported by RSF Grant No. 22-22-00333. M.M.R. acknowledges the funding provided by the Institute of Physics Belgrade through the grant by the Ministry of Education, Science, and Technological Development of the Republic of Serbia. Numerical simulations were run on the PARADOX supercomputing facility at the Scientific Computing Laboratory of the Institute of Physics Belgrade. The work in Florida was supported by NSF Grant No. 1822258 and the National High Magnetic Field Laboratory through the NSF Cooperative Agreement No. 1157490 and the State of Florida. The NTU group acknowledges support by the Ministry of Science and Technology, Taiwan (Projects No. 110-2622-8-002-014 and No. 110-2634-F-009-027). The Northeastern group was supported by NSF Grant No. 1904024.

Author contributions

This project was conceived, planned and executed by M.Yu.M., A.A.S., V.T.D. and S.V.K. Data were taken by M.Yu.M. and A.A.S. The SiGe/Si/SiGe wafers were grown by S.-H.H. and C.W.L. and processed by M.Yu.M. and A.A.S. The data analysis was made by M.Yu.M., A.A.S., V.T.D., A.Y.X.Z. and S.V.K. The manuscript was composed by A.A.S. and S.V.K. All the authors reviewed the manuscript.

Competing Interest

The authors declare no competing interests.

Additional information

Correspondence and requests for materials should be addressed to S.V.K.

Reprints and permissions information is available at www.nature.com/reprints.

Publisher's note Springer Nature remains neutral with regard to jurisdictional claims in published maps and institutional affiliations.



Open Access This article is licensed under a Creative Commons Attribution 4.0 International License, which permits use, sharing, adaptation, distribution and reproduction in any medium or format, as long as you give appropriate credit to the original author(s) and the source, provide a link to the Creative Commons licence, and indicate if changes were made. The images or other third party material in this article are included in the article's Creative Commons licence, unless indicated otherwise in a credit line to the material. If material is not included in the article's Creative Commons licence and your intended use is not permitted by statutory regulation or exceeds the permitted use, you will need to obtain permission directly from the copyright holder. To view a copy of this licence, visit <http://creativecommons.org/licenses/by/4.0/>.

© The Author(s) 2022